Supporting Information

Metal-ion exsolution effect to accelerate the reaction kinetics in Li-S batteries

Hongxu Zhou,[a] Weichen Han,[a] Hongquan Chai,[a] Hao Huang,[a] Jingang Zheng,[a] Han Zhang,*[a] Lixiang Li[a], Weimin Zhou[a], Baigang An[a] and Chengguo Sun*[a,b]

[a] School of Chemical Engineering, University of Science and Technology, Anshan, Liaoning, 114051, China

[b] School of Chemical Engineering, Nanjing University of Science and Technology, Nanjing, Jiangsu, 210094, China

* Corresponding Author: Chengguo Sun (sunyangguo2004@163.com)

Supporting Figures:

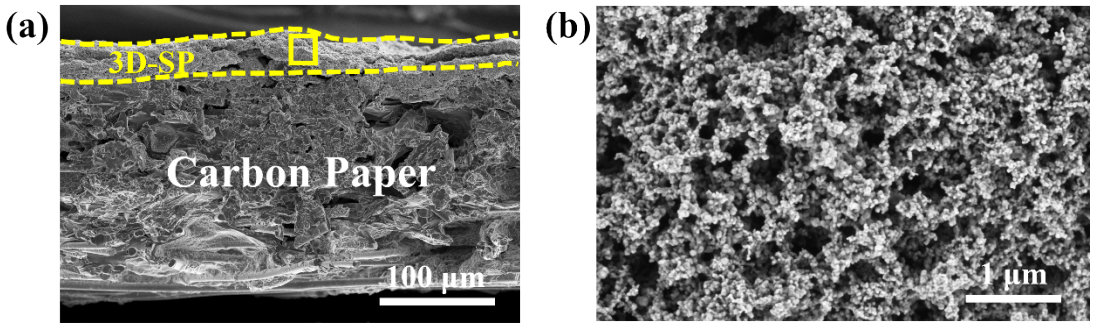

Fig. S1. (a) Cross-sectional SEM images of 3D-SP and (b) magnified SEM image of (a) with yellow box selected.

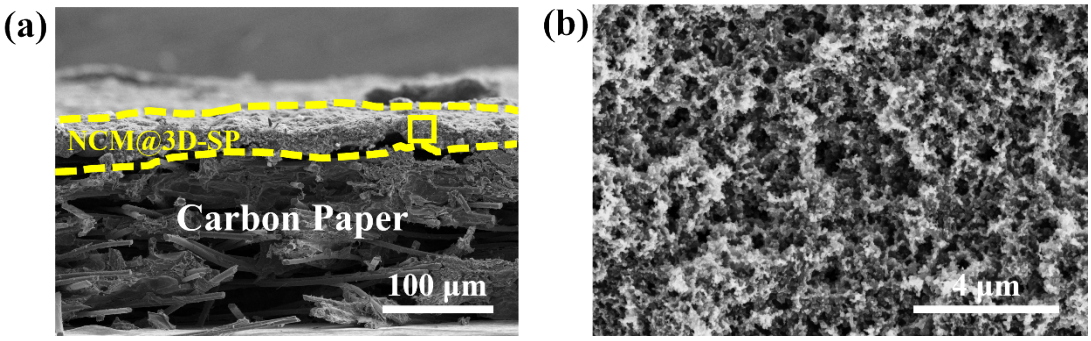

Fig. S2. (a) Cross-sectional SEM images of NCM@3D-SP and (b) magnified SEM image of (a) with yellow box selected.

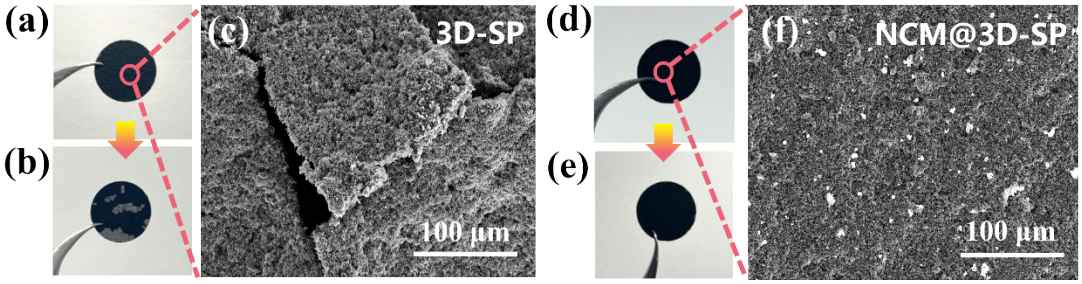

Fig. S3. (a) Digital picture of 3D-SP, corresponding to SEM (c), (b) after peeling test of the electrode. (d) Digital picture of NCM@3D-SP, corresponding to SEM (f), (e) after peeling test of electrode.

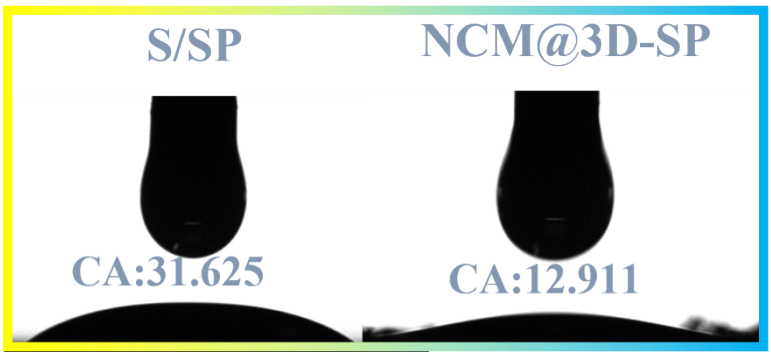

Fig. S4. Contact angle of different electrodes.

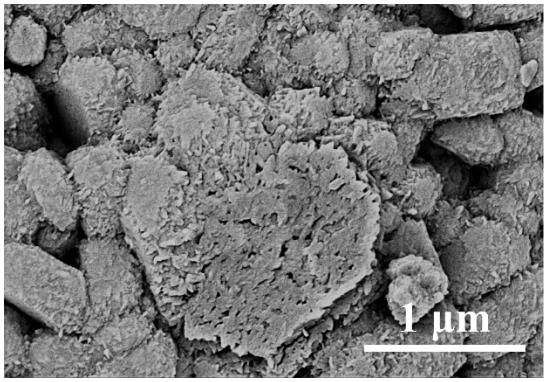

Fig. S5. SEM image of NCM811 after carbonization.

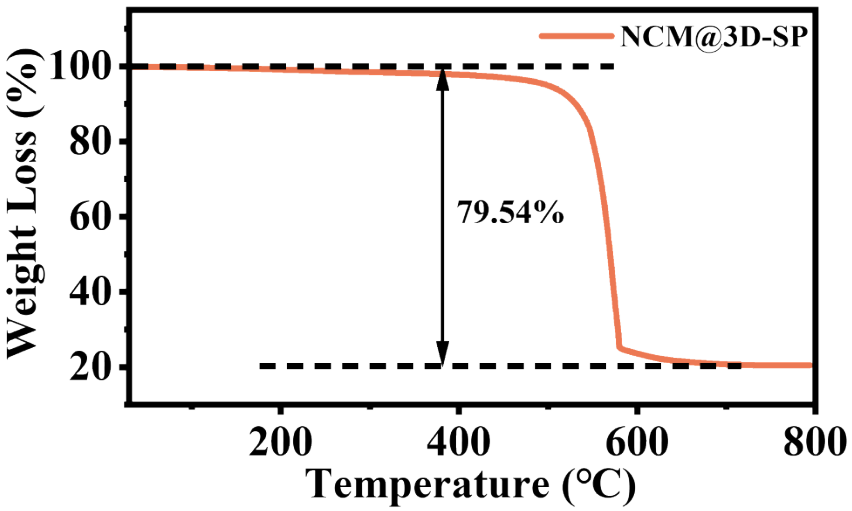

Fig. S6. TGA curve of NCM@3D-SP electrode.

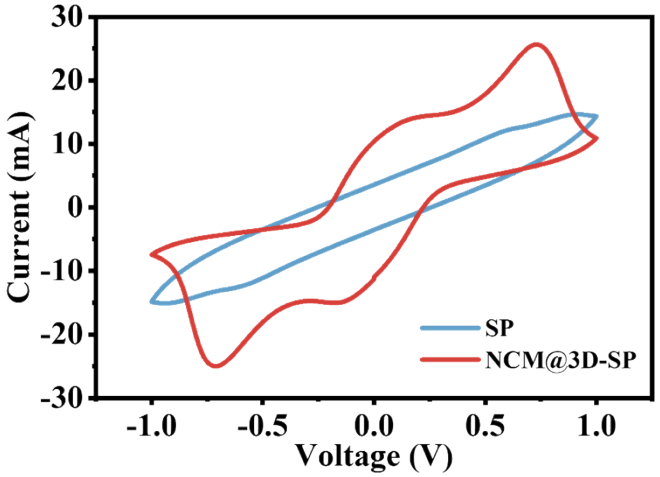

Fig. S7. Cyclic voltammetry profiles of Li_2S_6 symmetric cells of SP and NCM@3D-SP electrode.

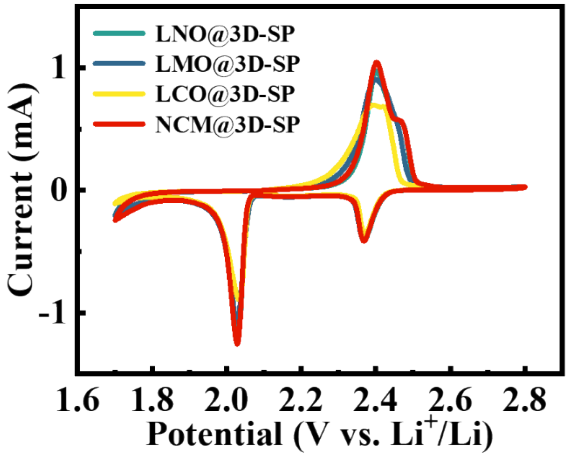

Fig. S8. CV curves of different electrodes at a scan rate of 0.1 mV s^{-1}.

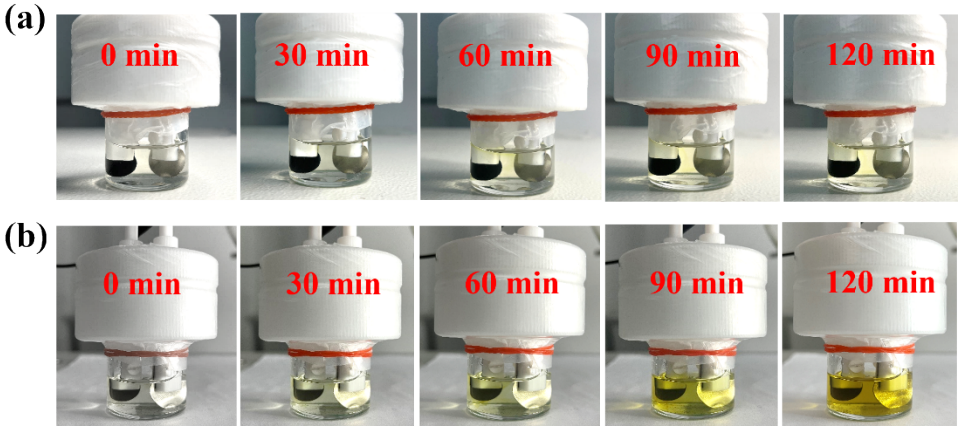

Fig. S9. Optical images of the glass bottle cells using (a) NCM@3D-SP/S and (b) S/SP as the cathodes at varied discharge time.

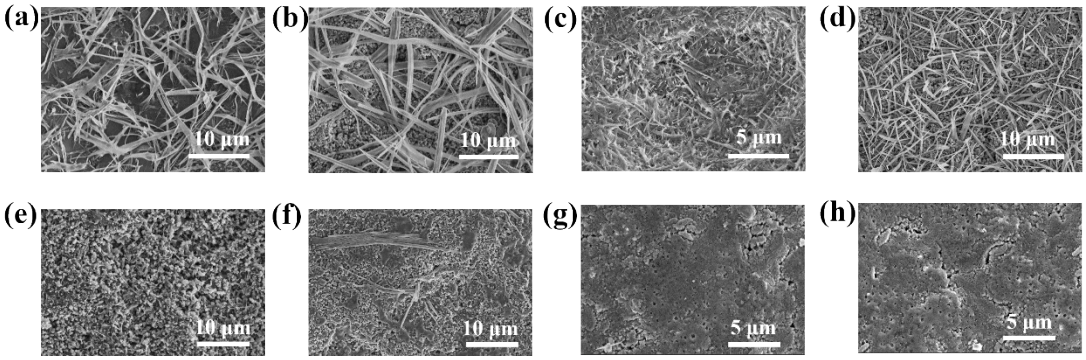

Fig. S10. Morphology characterization of (a-d) 3D-SP and (e-h) NCM@3D-SP after different cycles. (a,e) After 100th cycles; (b,f) after 200th cycles; (c,g) after 300th cycles, and (d,h)after 400th cycles.

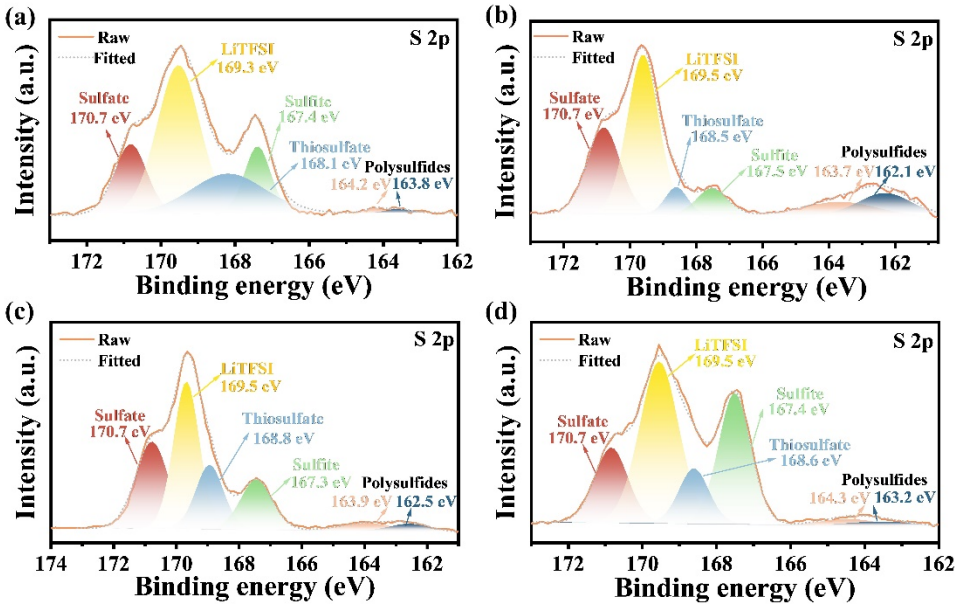

Fig. S11. S 2p XPS spectra of different separators with (a) NCM@3D-SP/S; (b) LMO@3D-SP/S; (c) LCO@3D-SP/S; (d) LNO@3D-SP/S cathodes after cycling.

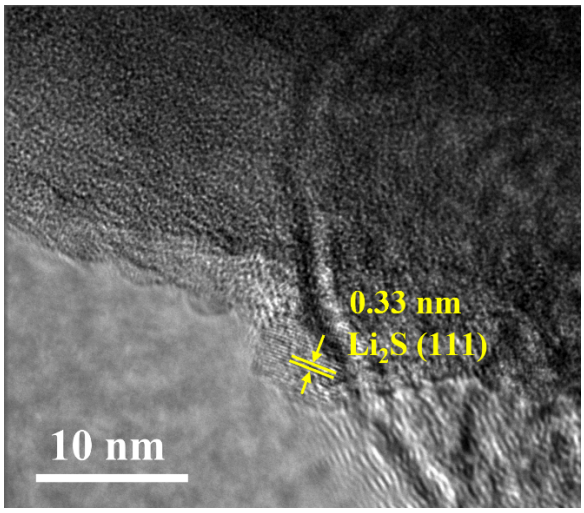

Fig. S12. HRTEM of the NCM@3D-SP/S cathode after 100 cycles at 0.2 C.

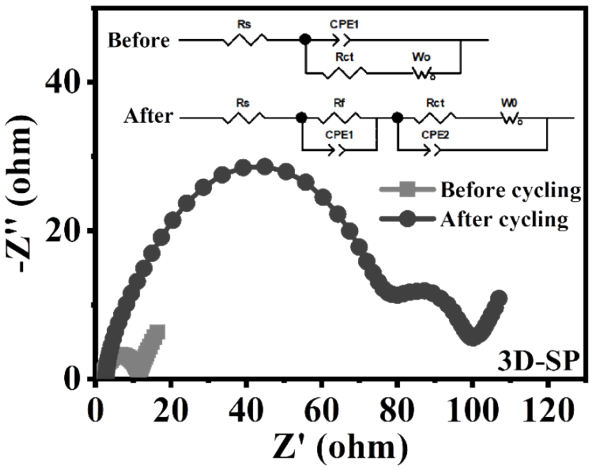

Fig. S13. EIS diagram of 3D-SP cathode.

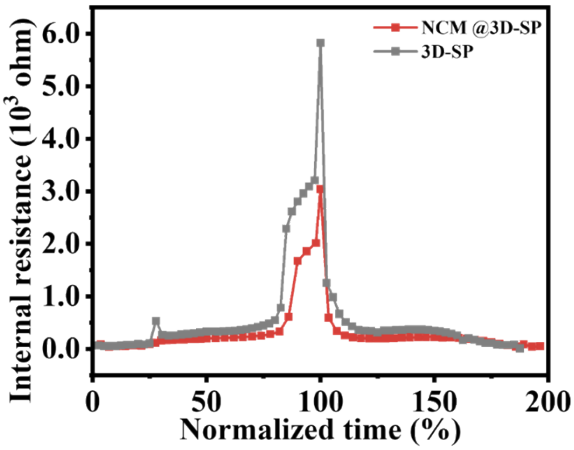

Fig. S14. The internal resistance of NCM@3D-SP and 3D-SP cathode relative to the normalized discharge-charge time.

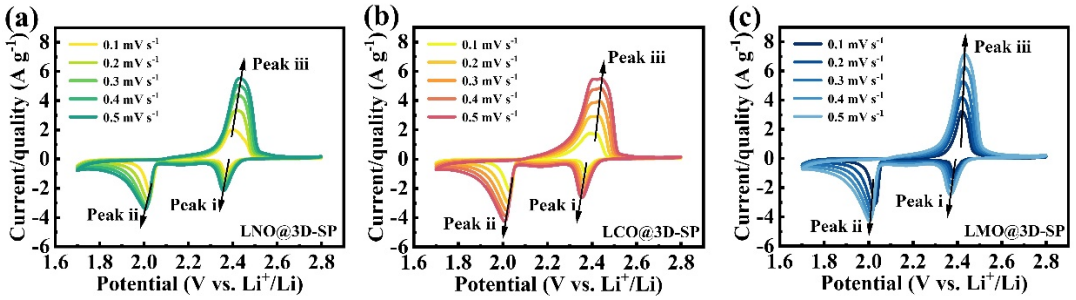

Fig. S15. CV profiles at different scan rates of (a) LNO@3D-SP, (b) LCO@3D-SP, and (c) LMO@3D-SP.

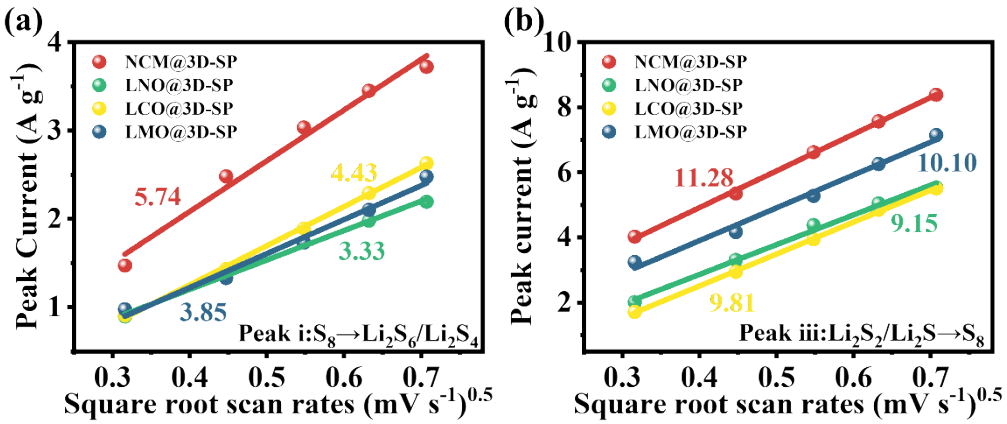

Fig. S16. I-$\upsilon^{-0.5}$ slope curves at (a) peak i and (b) peak iii.

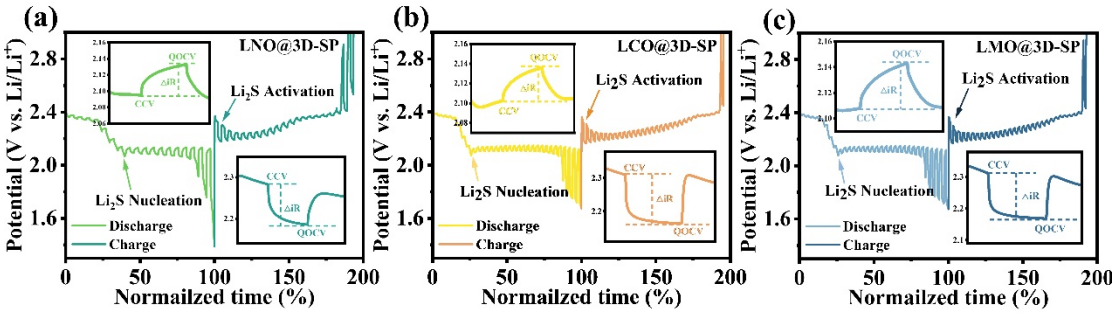

Fig. S17. GITT voltage profiles of (a) LNO@3D-SP, (b) LCO@3D-SP, and (c) LMO@3D-SP at 0.1 C.

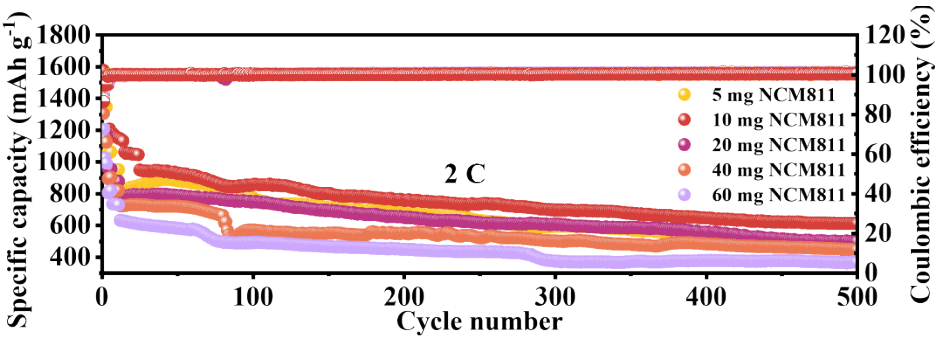

Fig. S18. Long-time cycling performance for Li-S cells with different amounts of NCM811 at 2 C.

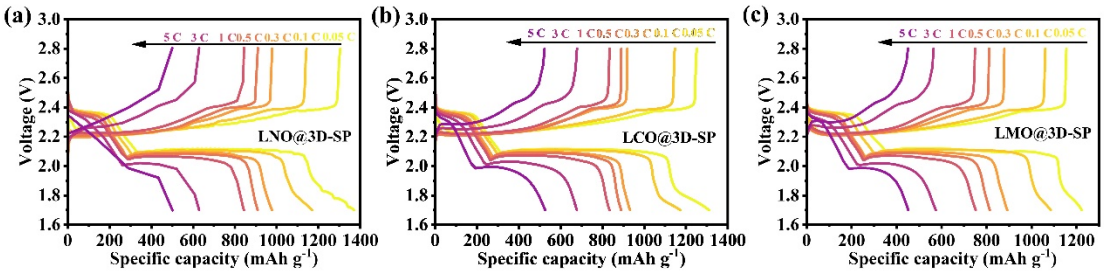

Fig. S19. Charge/discharge curves of (a) LNO@3D-SP, (b) LCO@3D-SP, and (c) LMO@3D-SP at different rate capability.

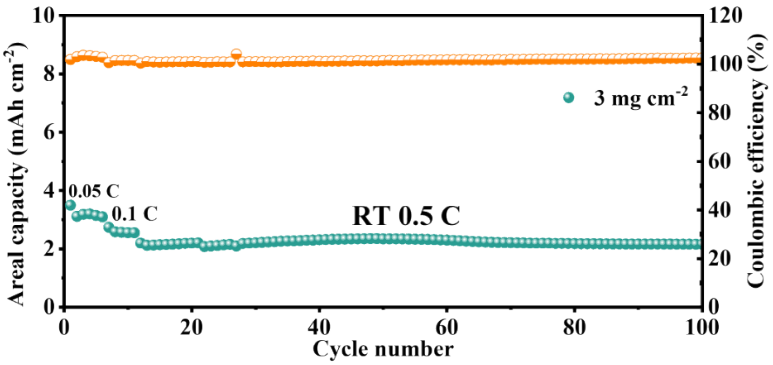

Fig. S20. The areal capacity of NCM@3D-SP with a sulfur loading of 3 mg cm^{-2} at 0.5 C.

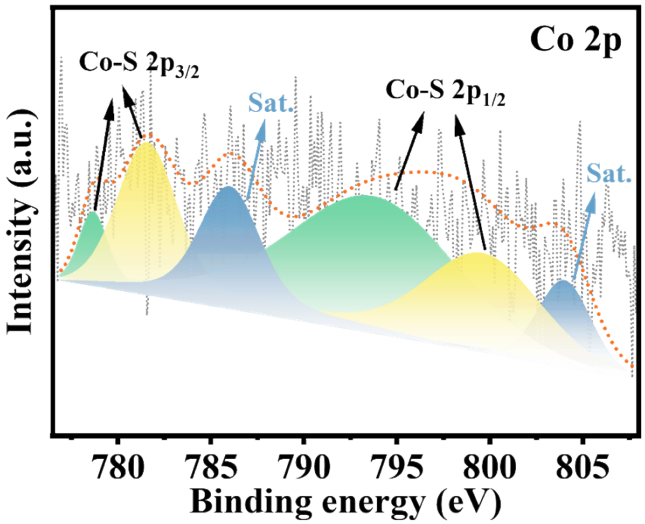

Fig. S21. Co 2p XPS spectra of NCM@3D-SP/S cathode after 200 cycles.

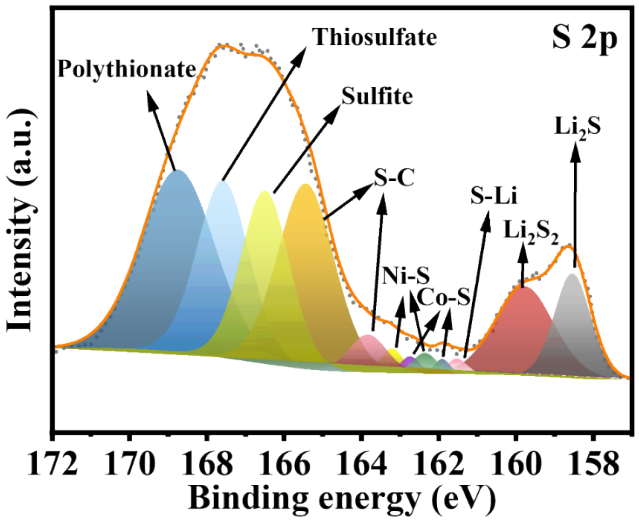

Fig. S22. S 2p XPS spectra of NCM@3D-SP/S cathode after 200 cycles.

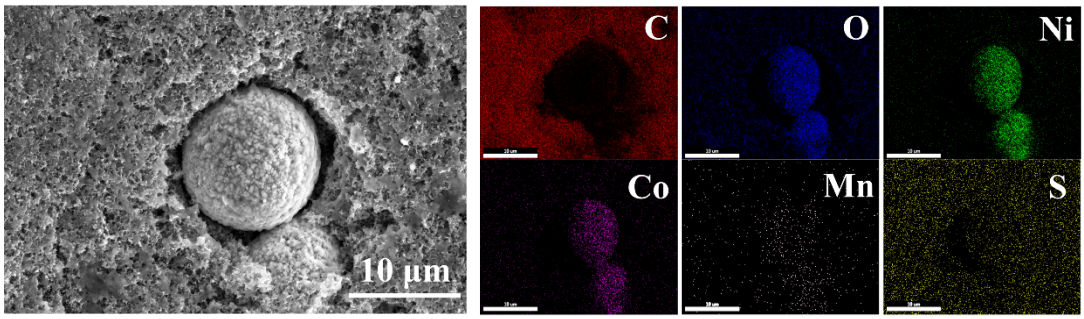

Fig. S23. SEM image and EDX elemental mappings of NCM particles in NCM@3D-SP/S cathode after 100 cycles at 0.5 C.

Supporting Tables:

Table S1. Fitted values of resistances in the equivalent circuit before cycling.

	Electrode	R_s/ Ω	R_{ct}/ Ω
Before cycle	LNO@3D-SP	1.73	79.47
	LCO@3D-SP	9.37	92.09
	LMO@3D-SP	1.67	98.81
	NCM@3D-SP	2.14	57.15

Table S2. Fitted values of resistances in the equivalent circuit after cycling.

	Electrode	R_s/ Ω	R_{ct}/ Ω	R_f/ Ω
After cycle	LNO@3D-SP	2.10	8.46	4.65
	LCO@3D-SP	1.85	7.71	6.80
	LMO@3D-SP	11.33	27.79	9.53
	NCM@3D-SP	3.75	6.69	2.04

Table S3. Fitting values of σ and D_{Li+} for different cathodes.

Electrode	σ	D_{Li+}/ 10^{-11} (cm^2 s^{-1})
LNO@3D-SP	19.79	4.07
LCO@3D-SP	16.57	5.81
LMO@3D-SP	17.78	5.04
NCM@3D-SP	14.24	7.86

Table S4. Fitted values of resistances in the equivalent circuit of the 3D-SP//Li battery.

Electrode	State	R_s/ Ω	R_{ct}/ Ω	R_f/ Ω
3D-SP	Before cycling	2.35	9.15	
	After cycling	2.83	37.75	77.86

Table S5. Fitting values of σ and D_{Li+} for 3D-SP electrode.

Electrode	σ	D_{Li+}/ 10^{-11} (cm^2 s^{-1})
3D-SP	22.78	3.07

Table. S6 Electrochemical performance of the Li-S batteries with various cathodes.

Composites	S loading (mg cm^{-2})	Discharge capacity (mAh g^{-1})	Capacity decay per cycle (%)	Current density (C)	Cycle number	Ref.
NCM@3D-SP/S	**1~1.3**	**649.5 (5 C)** **453.1 (10 C)**	**0.051**	**2**	**500**	This work
Co─MnO@CF	3	904 (0.5 C) 707 (4 C)	0.058	1 C	400	[1]
S/SG-1400	3.5	1442 (0.2 C) 857 (4 C)	0.067	2	500	[2]
DAAQ-COF@S	1.2	1182 (0.1 C) 618 (4 C)	0.27	0.1	100	[3]
S@rGO-rGO	1.5	975.4 (0.2 C) 797.7 (0.5 C)	0.058	0.5	400	[4]
CC@i-CMO/S	2	962 (0.5 C) 728 (2 C)	0.11	1	400	[5]
$ZnCo_2O_4$@Ti_3C_2 /S	1~1.5	1015 (0.2 C) 429.3 (1 C)	0.183	0.5	400	[6]
NC@TiO2-CNTs/S	1	1527 (0.2 C) 663 (5 C)	0.056	1 C	500	[7]
Pt/CS/S	1.2	459.7 (0.5 C)	0.121	0.2	500	[8]
S/3DOM Ta/N-TiO_2@Co-NC	1.5	1142 (0.3 C) 789.4 (5 C)	0.06	1	500	[9]
Pt/NCS/S	1.2	1063 (0.2 C) 422.6 (2 C)	0.13	0.2	500	[10]
S@C-$NiCo_2O_4$/PC	1.5~2.0	746.2 (0.5 C) 593.6 (2 C)	0.053	0.5	500	[11]
Fe_3O_4/FeP@C─S	1~1.2	1304 (0.2 C) 1093 (1C)	0.28	0.2	100	[12]

PTS/VSGC	1.4	514 (1 C) 413.2 (6 C)	0.08	0.5	500	[13]
CoS_2@NSC/S	1~1.2	1459 (0.1 C) 803 (3 C)	0.069	0.2	300	[14]
SN-CoSn@C NBs/S	1	557.3 (5 C)	0.076	1	500	[15]
Ni/Ni_3N–CNT/S	1.2	829.4 (0.5 C) 647.6 (5 C)	0.1	5	400	[16]
S@VN/Co_3ZnC @NCNT	1~1.2	639.2 (0.2 C) 566.4 (5 C)	0.064	1	500	[17]

References:

1 H. Zhu, S. Chen, X. Yao, K. Yang, W. Zhao, T. Chen, L. Yang and F. Pan, *Adv. Funct. Mater.*, 2024, 2401470.

2 F. Zhou, Y. Meng, T. Wang, D. Sun, L. Gao, Z. Sun, Y. Wang, J. Zeng, B. Wang, R. Zhang, R. Li, C. Huang, L. Yang and X. Wang, *Nano Energy*, 2024, **127**, 109755.

3 S. Cai, R. Ma, W. Ke, H. Zhang, Y. Liu, M. Jiao, Y. Tian, Y. Fang, M. Wu and Z. Zhou, *Chem. Eng. J.*, 2024, **491**, 151979.

4 Z. Li, J. Liu, T. Wang, J. Zhu, C. Cheng, G. Ao, Z. Guan and J. Zhu, *Carbon*, 2024, **222**, 118966.

5 X. Huang, P. Zeng, Y. Lu, J. Yang, M. Chen, H. Liu and X. Wang, *Chem. Eng. J.*, 2024, **487**, 150490.

6 Z. Li, J. Liu, T. Wang, J. Zhu, C. Cheng, G. Ao, Z. Guan and J. Zhu, *Carbon*, 2024, **222**, 163369.

7 B. Yue, L. Wang, N. Zhang, Y. Xie, W. Yu, Q. Ma, J. Wang, G. Liu and X. Dong, *Small*, 2023, **20**, 2308603.

8 Y. Qi, N. Chai, Q. Gu, J. Chen, M. Lu, X. Zhang and B. Zhang, Chem. Eng. J., 2022, **435**, 135112.

9 C. Xu, S. Zheng, J. Guo, D. Sun, Z. Zhang and J. Li, *Chem. Eng. J.*, 2023, **463**, 142295.

10 Y. Qi, N. Chai, Q. Gu, J. Chen, Z. Zhai, M. Lu, Y. Niu, N. Huang, X. Zhang and B. Zhang, *J. Energy Chem.*, 2023, **87**, 123-135.

11 L. Bai, Z. Guan, J. Nie and B. Du, *Chem. Eng. J.*, 2023, **466**, 143187.

12 J. Li, Z. Wang, K. Shi, Y. Wu, W. Huang, Y. Min, Q. Liu and Z. Liang, *Adv. Energy Mater.*, 2023, **14**, 2303546.

13 P. Zhang, Y. Fu and W. Guo, *Small*, 2023, **19**, 2207047.

14 M. Zheng, J. Zhao, W. Wu, R. Chen, S. Chen and N. Cheng, *Small*, 2023, **20**, 2303192.

15 R. Gao, Q. Zhang, H. Wang, X. Wang, J. Ren and R. Wang, *J. Mater. Chem. A*, 2022, **10**, 23254-23264.

16 T. Xiao, F. Yi, H. Wang, M. Yang, W. Liu, M. Ren, X. Zhang and Z. Zhou, *J. Mater. Chem. A*, 2022, **10**, 16866-16872.

17 J. Fu, Z. Shen, D. Cai, B. Fei, C. Zhang, Y. Wang, Q. Chen and H. Zhan, *J. Mater. Chem. A*, 2022, **10**, 20525-20534.